applied sciences

MDPI

Article

Modal Analysis–Based Characterization of the Material Properties of a Sawbones Composite Vertebra Model

Marthe Van den Bogaert [1,*], Henrique Duarte Vieira de Sousa [2,3,*], Maikel Timmermans [1,3], Konstantinos Gryllias [2,3] and Kathleen Denis [1]

[1] Smart Instrumentation Research Team, Division of Biomechanics, Department of Mechanical Engineering, KU Leuven, 3001 Leuven, Belgium; maikel.timmermans@kuleuven.be (M.T.); kathleen.denis@kuleuven.be (K.D.)
[2] LMSD—Mecha(tro)nic System Dynamics, Department of Mechanical Engineering, KU Leuven, 3001 Leuven, Belgium; konstantinos.gryllias@kuleuven.be
[3] Flanders Make@KU Leuven, 3001 Leuven, Belgium
* Correspondence: marthe.vandenbogaert@kuleuven.be (M.V.d.B.); henriqueduarte.vieiradesousa@kuleuven.be (H.D.V.d.S.)

Abstract

Composite bone replicas are widely used in biomechanical testing as alternatives to cadaveric specimens, with numerical models often complementing or replacing experiments. The reliability of these models depends strongly on accurate material parameters. This study investigates a fourth-generation Sawbones composite L5 vertebra, updating cortical material properties under isotropic and transversely isotropic modelling assumptions. Finite element models were calibrated using free-free experimental modal analysis, revealing differences between manufacturer-provided material properties and the measured specimen behaviour. For both models, matching the specimen mass required reducing the cortical density from 1.64 g/cm^3 to 1.423 g/cm^3. In the isotropic model, the Young's modulus was reduced from 16,000 MPa to 6500 MPa. In the transversely isotropic model, longitudinal and transverse Young's moduli were reduced from 16,000 MPa and 11,000 MPa to 6400 MPa and 5500 MPa, respectively, while the shear moduli decreased from 4370 MPa and 6350 MPa to 3500 MPa and 2540 MPa. In both models, the Poisson's ratio was increased from 0.26 to 0.30. These updates reduced the average eigenfrequency error to 6.12% (isotropic) and 5.83% (transversely isotropic), with the first five modes errors reduced to 3.10% and 2.80%, respectively, substantially improving numerical representation of L5 vertebral mechanics. The updated vertebral FE model and accompanying workflow enhance the reliability of future FE analyses, improve interpretation of Sawbones vertebra biomechanical results, and support vibration-based biomechanical applications such as implant fixation assessment.

Keywords: vertebra; replica composite bone; material parameters updating; modal analysis; finite element model

Check for updates

Academic Editor: Hossein Bisheh

Received: 23 January 2026
Revised: 24 February 2026
Accepted: 26 February 2026
Published: 3 March 2026

Copyright: © 2026 by the authors. Licensee MDPI, Basel, Switzerland. This article is an open access article distributed under the terms and conditions of the Creative Commons Attribution (CC BY) license.

1. Introduction

Composite replica bone models are artificial analogues of cadaveric bones, designed to approximate the mechanical behaviour of human bones for biomechanical testing. They offer an alternative with low inter-specimen variability to cadaveric material, which is more difficult to obtain, more demanding in handling and storage, and less repeatable [1–3]. A widely used example of such composite replica bone models in biomechanical research is

the Sawbones line (Pacific Research Laboratories, Vashon, WA, USA), consisting of a hard composite (short-fibre-filled epoxy resin) shell and a polyurethane foam core. Extensive research has confirmed that Sawbones exhibit mechanical properties that realistically mimic those of cadaveric bones [4]. Typical applications include the evaluation of fracture fixation constructs, assessment of orthopedic implant performance, and simulation of complex fracture geometries [3,5].

Finite element (FE) analysis has become an essential tool in biomechanical research, serving both as an alternative and a complement to experimental testing [6–8]. FE simulations allow investigation of loading scenarios or boundary conditions that cannot be reproduced in laboratory settings. Additional advantages include the ability to systematically modify geometry and material properties so that analyses can capture the full range of patient variability. Composite bones are frequently used as the basis for FE models and as experimental benchmarks for validating computational predictions [9–12]. Reliable FE analysis requires accurate assignment of material properties. Such properties are commonly derived from mechanical tests on the physical bone models, including tensile and three-point bending tests [13]. However, obtaining these properties is not always straightforward—particularly for composite structures with complex geometries. Variations in cross-sectional area and internal material distribution make deriving global material properties through simple mechanical tests practically infeasible. An alternative, non-invasive approach is to use modal analysis to determine dynamic characteristics and update FE model material properties by minimizing differences between experimental and simulated modal parameters [14]. This approach has been applied, for example, to determine the material properties of concrete structures [15] and to characterize Sawbones models such as a replica femur [16] and clavicle [17].

The present study focuses on the L5 vertebra model. Material properties reported by Sawbones in their datasheet [18,19] are based on mechanical testing of a flat sheet of short-fibre-filled epoxy. Because Sawbones composite models are manufactured via injection moulding, fibre orientation is influenced by flow patterns during processing. It is well established that controlling fibre orientation becomes increasingly difficult in components with complex geometries [20]. Therefore, the aim of this study is to evaluate whether the material properties of the Sawbones vertebra model align with those specified in the datasheet. Deviations are expected due to the flow-dependent fibre orientation in the intricate vertebral geometry, which cannot be controlled as precisely as in a flat sheet. Previous studies [16,17] have already shown substantial deviations between datasheet values and actual material properties in more complex composite bone models. This motivates the current investigation for the vertebra model. Sawbones vertebra models are widely used in biomechanical research [21,22]. Ensuring that future experimental and computational studies rely on accurate material properties is essential, since the interpretation of results depends heavily on the assumption that the model's material parameters are correctly defined.

Accordingly, this study applies experimental and numerical modal analysis to a Sawbones composite vertebra model to investigate whether the manufacturer's datasheet-based material properties remain valid for complex vertebral geometries. A short verification study on a sheet model was also included (Sections 2.5 and 3.1). This was done to ensure that the proposed workflow reproduces expected bulk properties when applied to the product for which the material properties in the datasheet were derived.

2. Materials and Methods

2.1. Composite Bone Model

This study evaluated a fourth-generation composite L5 vertebra model (Sawbones Model 3429-5-2, Sawbones, Vashon Island, WA, USA) [23], as shown in Figure 1. The bone model comprises two distinct material layers: a cortical bone analogue made from absolute^{TM} fourth-generation glass fibre–reinforced epoxy (outer shell), and a cancellous bone analogue consisting of 10 PCF solid polyurethane (PU) foam (inner core). The composite bone model has a total mass of 46.35 g, as measured using a precision scale (Kern PFB 300-3N, Kern & Sohn GmbH, Balingen-Frommern, Germany).



Figure 1. Sawbones absolute^{TM} fourth-generation lumbar L5 vertebra model with 10 PCF solid foam cancellous core (3429-5-2).

2.2. Finite Element Model

The three-dimensional geometry of the Sawbones L5 vertebra was obtained from a CT scan acquired with a slice thickness of 0.6 mm using a Somatom Force scanner (Siemens Healthineers AG, Forchheim, Germany) at UZ Leuven. The CT data were imported into Mimics medical image processing software (Materialise NV, Leuven, Belgium), where cortical and cancellous bone analogue regions were segmented based on grayscale intensity values. The resulting segmented geometries were reconstructed into 3D models and exported as STL files, which served as the basis for the FE model.

In the FE model, the cortical and trabecular regions were discretized using separate meshes of quadratic tetrahedral elements. An optimal element size of 6 mm was obtained by performing a mesh convergence analysis. Figure 2 shows the FE model with the selected mesh size. Surface-to-surface glueing was applied between both meshes. Two types of model updating were conducted. In both cases, the trabecular analogue was modeled as an isotropic material, whereas the cortical layer was assumed to be isotropic in one analysis and transversely isotropic in the other.

The isotropic elastic material model is fully characterized by two independent material parameters, for instance E (Young's modulus) and ν (Poisson's ratio). In contrast, the transversely isotropic elastic material model requires five independent constants: $E_1 = E_2$ (transverse Young's moduli), E_3 (longitudinal Young's modulus), $\nu_{12} = \nu_{23} = \nu_{13}$, G_{12} and $G_{13} = G_{23}$. The plane of isotropy ($E_1 = E_2$) corresponds to the transverse plane of the vertebra (1–2 plane in Figure 2), whereas the longitudinal material direction (E_{33}) is aligned with the anatomical axis of the vertebra (axis 3 in Figure 2) and is perpendicular to this plane of isotropy. The initial material properties used in the numerical model were derived from technical reports provided by the manufacturer of the bone replica [18,19,24], and are summarized in Table 1. Since the Poisson's ratio of the cancellous bone is not provided by the manufacturer, a value of $\nu = 0.3$ was adopted from the literature [4]. Assuming isotropy in the 1–2 plane and extending an isotropic approximation to the

1–3 and 2–3 planes, the shear moduli for the cortical bone in the transverse isotropic model were estimated assuming

$$G_{12} = \frac{E_1}{2(1+\nu_{12})}, \quad (1)$$

and

$$G_{13} = G_{23} = \frac{E_3}{2(1+\nu_{13})}. \quad (2)$$

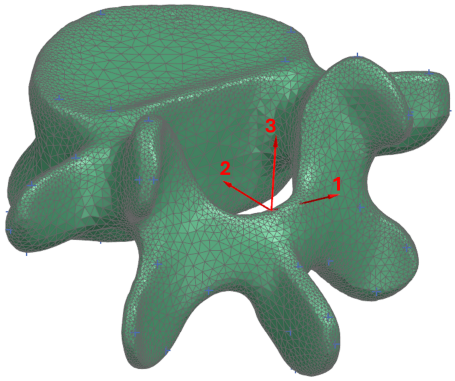

Figure 2. FE model of the Sawbones L5 vertebra with a CTETRA10 6 mm mesh. The axes 1 and 2 represent the transverse plane of the vertebra, while axis 3 is aligned with the vertical anatomical axis of the vertebra.

Table 1. Initial material properties as derived from [4,18,19,24] for the isotropic and transversely isotropic FE models of the composite L5 vertebra.

Initial Material Parameters			
Cancellous			
ISOTROPIC	E [MPa]	ν	ρ [g/cm^3]
	86	0.30	0.16
Cortical			
ISOTROPIC	E [MPa]	ν	ρ [g/cm^3]
	16,000	0.26	1.64
TRANSVERSELY ISOTROPIC	$E_1 = E_2$ [MPa]	E_3 [MPa]	ρ [g/cm^3]
	11,000	16,000	1.64
	G_{12} [MPa]	$G_{23} = G_{13}$ [MPa]	$\nu_{12} = \nu_{23} = \nu_{13}$
	4370	6350	0.26

2.3. Experimental Modal Analysis

An experimental modal analysis was performed on the vertebra model to determine its dynamic characteristics. To ensure consistency with the FE simulations and to allow for unrestricted motion, free–free boundary conditions were approximated by suspending the vertebra using elastic cords. The suspension points were chosen at the pedicles to minimize the influence of the suspension system on the measured dynamics, as these regions exhibit high structural stiffness and coincide with nodal points of the vibration modes. A total of 44 measurement points were defined on the composite vertebra, consisting of 41 excitation points and 3 response points, as illustrated in Figure 3. The structure was excited using a manual impact hammer equipped with a force cell and a stainless steel hammer tip (PCB 086C03, PCB Piezotronics, Depew, NY, USA). The excitation points were evenly distributed over the test object in three mutually perpendicular directions to ensure adequate global modal excitation. As the vertebral processes, the irregular shapes at the backside of the

vertebra, are of particular interest due to their pronounced local modal behaviour, a higher density of excitation points was introduced in these regions to enable a more detailed characterization of the local bending and torsional behaviour. Excitation points were placed near anti-nodes of the expected mode shapes, where vibration amplitudes are highest, in order to maximize modal participation. Furthermore, the excitation directions were chosen to align with the dominant displacement components of the corresponding modes, to ensure efficient excitation of the targeted modes. The vibration response was measured using three lightweight uniaxial accelerometers (PCB 352A24, PCB Piezotronics, Depew, NY, USA, mass 0.8 g) that were mounted on the vertebra in three orthogonal directions using beeswax. Figure 4 shows the instrumentation of the composite vertebra. Five measurements were averaged for each excitation location. Data acquisition and signal conditioning were performed using a Simcenter SCADAS Mobile data acquisition system equipped with V8 modules (Siemens, Leuven, Belgium), in combination with Simcenter Testlab modal analysis software (Simcenter Testlab Impact Testing 2406, Siemens PLM Software, Leuven, Belgium). An exponential input window was applied to improve the quality of the frequency spectra, and 1024 spectral lines were selected to balance acquisition time and frequency resolution. The acquisition bandwidth was set to 8192 Hz, based on the frequency range identified in the numerical modal analysis and on observations of the input power spectral density. This configuration resulted in a dataset comprising 129 frequency response functions (FRFs), computed using the H1 estimator. Modal parameters, including resonance frequencies and mode shapes, were extracted from the FRFs using the PolyMAX algorithm implemented in Simcenter Testlab, over a frequency range from 1000 to 8192 Hz.

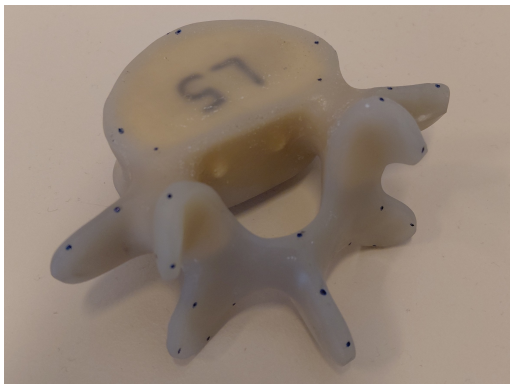

Figure 3. Excitation points on the composite vertebra.

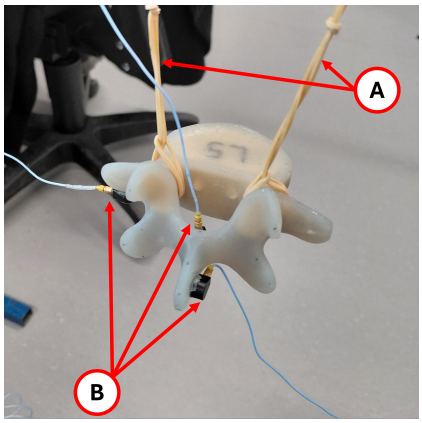

Figure 4. Experimental test setup showing the vertebra model suspended by elastic cords (A) and instrumented with three orthogonally oriented uniaxial accelerometers (B).

2.4. FE Parameter Updating

The purpose of the model updating procedure is to improve the predictive accuracy of the FE model of the composite vertebra by correlating and matching its first ten vibration modes with those identified through experimental modal analysis. This process involves minimizing discrepancies in natural frequencies and mode shapes, thereby ensuring that the updated model accurately represents the dynamic behaviour of the physical vertebra replica.

Although ten modes were identified within the investigated frequency range, the updating procedure primarily targeted the first five modes as their higher excitation energy density resulted in more reliable experimental identification, and consequently, greater updating accuracy.

The isotropic and the transverse isotropic model were updated separately and initially parametrized using elastic material properties derived from technical documentation provided by the manufacturer of the vertebra replica. To minimize the discrepancy between the measured mass of the vertebra replica and the mass of the FE model, the cortical analogue density was updated in a first step to match the physical mass. This density modification should be interpreted as a combined effective parameter rather than a pure material property update, as it simultaneously compensates for uncertainties in the material data and potential segmentation inaccuracies of the reconstructed cortical shell. Subsequently, the elastic material properties of the numerical models were updated through an iterative process similar to that of [17] to minimize the error between the corresponding experimentally measured and numerically predicted modal frequencies and mode shapes. For each iteration step, a numerical modal analysis of the FE model was performed using Simcenter Nastran to determine the resonance frequencies and mode shapes for the first ten modes, which were compared to the experimental results. The Modal Assurance Criterion (MAC), which provides a quantitative measure of mode shape correlation, was used to pair numerical and experimental mode shapes to ensure correct mode correspondence. At each iteration, the relative frequency errors and MAC values were evaluated.

A sensitivity analysis was performed for both isotropic and transversely isotropic models to identify the parameters exerting the greatest influence on the eigenfrequencies and, consequently, those with the highest priority for updating. Sensitivities were calculated by applying a 10% change to an individual material parameter, monitoring the resulting change in the resonance frequencies of the numerical model and subsequently normalizing the observed frequency shifts by a factor of ten. The results of the initial sensitivity study after updating the density are shown in Tables 2 and 3 for the isotropic and transverse isotropic models, respectively. From those sensitivity analysis results, it was evident that the material properties of the cortical layer have a significantly stronger influence. Consequently, the updating procedure focused on refining this layer's material properties. Following each 15% modification of a parameter, the sensitivity analysis was reiterated to ensure consistency in updating the most sensitive parameters during each step.

For the isotropic model, first, the Young's modulus (E) of the cortical layer was optimized in order to minimize the error between the corresponding experimental and numerical modal frequencies. This is reasonable as previous studies on other anatomical Sawbones bone replicas [16,17] have shown that the effective stiffness properties of the cortical bone analogue often differ substantially from their reported values and usually require considerable adjustment during FE model updating. In a final step, the Poisson's ratio was adjusted to further improve the agreement between numerical and experimental results.

For the transverse isotropic model, all elastic constants of the cortical layer were considered for updating during the optimization process, while the material properties of the cancellous bone analogue were kept constant. Based on the sensitivity of the natural

frequencies to the individual material parameters (Table 3), the transverse Young's moduli $E_1 = E_2$ and the shear moduli $G_{23} = G_{13}$ have the strongest influence and were therefore updated in a first optimization step. Specifically, $E_1 = E_2$ predominantly affected modes 3 and 5, whereas $G_{23} = G_{13}$ had the largest influence on modes 1 and 2. In a subsequent step, G_{12} and E_3 were adjusted to ensure consistency with $G_{23} = G_{13}$ and $E_1 = E_2$, respectively. To further minimize the error, the Poisson's ratio ν was iteratively updated in a final optimization step until the average difference in resonance frequencies between the FE model and the experimental measurements was reduced to below 3% for the first five modes.

Table 2. Initial sensitivities of the isotropic FEM natural frequencies to variations in material properties (% frequency change per % material change).

Sensitivities [%/%]				
Mode	**Cortical**		**Cancellous**	
	E	ν	E	ν
1	0.47	−0.02	0.02	0.00
2	0.46	−0.03	0.03	0.00
3	0.45	−0.01	0.03	−0.01
4	0.47	−0.03	0.02	0.00
5	0.46	0.01	0.03	0.00
6	0.46	−0.01	0.03	−0.01
7	0.45	0.00	0.03	−0.01
8	0.47	0.00	0.02	0.00
9	0.40	0.01	0.07	−0.02
10	0.36	0.01	0.10	−0.03
Average sensitivity [%/%]	0.45	−0.01	0.04	−0.01

Table 3. Initial sensitivities of the transverse isotropic FEM natural frequencies to variations in material properties (% frequency change per % material change).

Sensitivities [%/%]							
Mode	**Cortical**					**Cancellous**	
	$E_1 = E_2$	E_3	$\nu_{12} = \nu_{23} = \nu_{13}$	G_{12}	$G_{23} = G_{13}$	E	ν
1	0.14	0.10	0.04	0.07	0.16	0.02	0
2	0.12	0.07	0.04	0.10	0.15	0.03	−0.01
3	0.19	0.06	0.05	0.06	0.13	0.04	−0.01
4	0.16	0.05	0.02	0.10	0.15	0.02	0
5	0.19	0.04	0.07	0.14	0.08	0.03	−0.01
6	0.10	0.09	0.06	0.10	0.15	0.03	−0.01
7	0.20	0.05	0.06	0.09	0.11	0.03	0
8	0.16	0.04	0.08	0.12	0.14	0.01	0
9	0.21	0.05	0.05	0.07	0.11	0.04	−0.01
10	0.13	0.06	0.06	0.10	0.12	0.05	−0.01
Average sensitivity [%/%]	0.16	0.06	0.05	0.09	0.13	0.03	−0.01

2.5. Verification of Datasheet Material Properties

Prior to analysing the vertebra model, the same modal testing and FE updating procedure was carried out on a Sawbones absolute™ fourth-generation 4 mm thick sheet (Sawbones Model 3401-03, Sawbones, Vashon Island, WA, USA). It is for this type of sample that the material properties in the Sawbones datasheet were derived by standardized mechanical testing. The verification measurements were done to ensure that the implemented workflow reproduces expected bulk properties for simple geometries corresponding to

the official datasheet. Section 1 already stated the hypothesis that the material properties of the vertebra model could potentially differ from those listed in the datasheet, as the flow-dependent fibre orientation in the intricate vertebral geometry cannot be controlled as precisely as in a flat sheet.

The composite sheet was freely supported on a light foam to simulate free-free boundary conditions. An automatic modal hammer (vImpact-61, Maul-Theet GmbH, Berlin, Germany) excited the sheet at each of the 30 measurement points, following the roving hammer principle. A laser vibrometer (IVS-500, Polytec GmbH, Waldbronn, Germany) measured the dynamic response of the sheet at one corner measurement point covered with thin reflective tape (see Figure 5). A corner point was selected for response measurement due to its large vibration amplitude in all modes of interest.

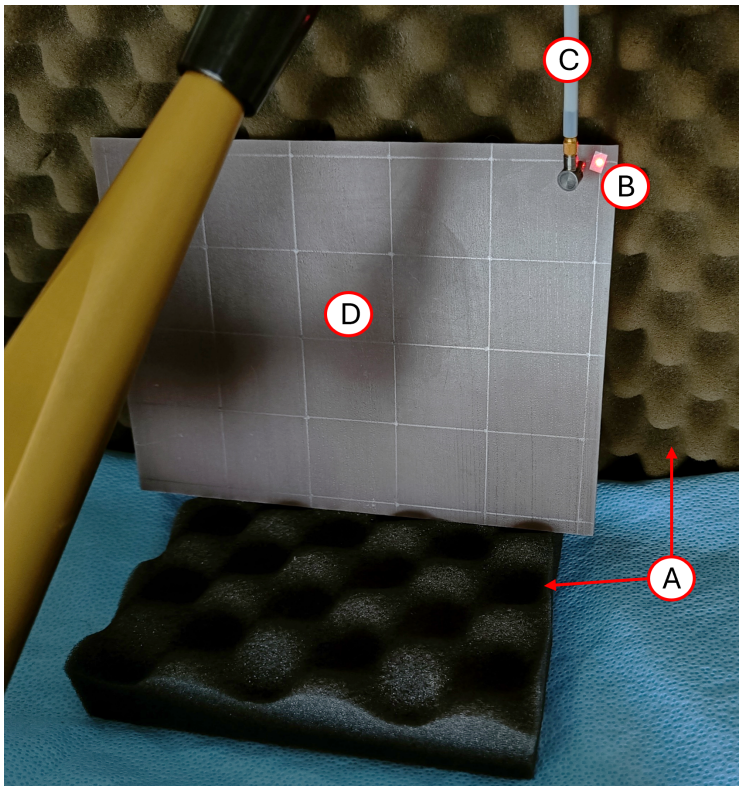

Figure 5. Experimental setup for verification measurements on Sawbones Sheet Model 3401-03. The sheet (D) is supported by light foam (A) to impose free-free boundary conditions. The response is measured by a laser vibrometer via a laser spot pointed to reflective tape (B) on the sheet. The plate was excited by an automatic modal hammer (C).

It is noteworthy that there are differences to the setup for the vertebra model, detailed in Section 2.3. First of all, the sheet is supported by light foam instead of rubber bands. This was done because the rubber bands could not contain the sheet properly. Regardless, both support methods have such low stiffness that the rigid-body support modes are at a frequency of at least 30 times lower than the first elastic mode and thus both effectively behave as free boundary conditions [25]. Second, a laser vibrometer is used to measure the response instead of lightweight accelerometers. When mass loading effects of an accelerometer are negligible, usage of laser vibrometers and accelerometers will lead to the same results in modal analysis [26,27]. In this case, a laser vibrometer was easier to use and eliminated even the smallest mass loading. Finally, an automatic modal hammer was used instead of a manual modal hammer. Modal parameters such as frequencies are not influenced by the type of hammer but automatic modal hammers lead to higher repeatability and sped up the measurement process for this simple plate geometry. All

software settings and procedures for measurements and simulations were the same as in Sections 2.3 and 2.4 except for a mesh size of 2 mm in the FE model.

3. Results

3.1. Verification with Sheet Model

Table 4 presents the final results for the experimental modal analysis and for the FE updating process with respect to the Sheet model. A good correspondence between experimental and numerical model is achieved with an average error over 8 modes of 0.88%.

Table 4. Obtained results of the eigenfrequencies for experimental modal analysis (EMA) and FE model after parameter updating for the Sawbones Sheet.

	Mode Number	**1**	**2**	**3**	**4**	**5**	**6**	**7**	**8**
EMA	Frequency [Hz]	289.52	320.14	666.46	800.35	1006.60	1234.13	1452.96	1749.34
FE	Frequency [Hz]	289.16	318.93	670.26	786.79	1017	1248	1448	1780
	Error [%]	−0.13	−0.38	0.57	−1.69	1.03	1.12	−0.34	1.75

Table 5 presents the updated material properties for the Sheet model. Very little updating was required compared to the material properties listed in the datasheet, which correspond to the values found in Table 1. It should be noted that for the Shear moduli, the initial values from previous literature were used [16,17], namely 3300 MPa, and not the initial values that in present study were calculated for the vertebra model in Equations (1) and (2). $E_1 = E_2$ was decreased by 5% and G_{12} was increased by 35%.

Table 5. Material parameters after updating the FE model for the Sawbones Sheet.

Material Parameters	
	After Updating
$\rho_{cortical}$ [g/cm^3]	1.640
TRANSVERSELY ISOTROPIC	
$E_1 = E_2$ [MPa]	10,400
E_3 [MPa]	16,000
G_{12} [MPa]	4455
$G_{13} = G_{23}$ [MPa]	3300
$\nu_{12} = \nu_{13} = \nu_{23}$	0.260

3.2. Vertebra Model

The resulting updates to the material parameters are summarized in Table 6, which provides an overview of all the modified properties. To match the mass of the physical component, the density of the cortical layer was updated from 1.640 g/cm^3 to 1.423 g/cm^3 in the FE model, while the density of the cancellous layer was kept unchanged due to its negligible contribution to the total mass. For the isotropic model, the Young's modulus E was reduced by 59% (from 16,000 MPa to 6500 MPa), while the Poisson's ratio ν increased by approximately 15% (from 0.260 to 0.300). For the transverse isotropic model, the Young's moduli $E_1 = E_2$ and E_3 were reduced by 50% (from 11,000 MPa to 5500 MPa) and 60% (from 16,000 MPa to 6400 MPa), respectively. The shear moduli E_{12} and $G_{13} = G_{23}$ were decreased by approximately 20% (from 4370 MPa to 3500 MPa) and 60% (from 6350 MPa to 2540 MPa), respectively, while the Poisson's ratios $\nu_{12} = \nu_{13} = \nu_{23}$ were increased by approximately 15% (from 0.260 to 0.300).

Table 6. Material parameters before and after updating the FE models.

Material Parameters		
	Before Updating	**After Updating**
$\rho_{cortical}$ [g/cm^3]	1.640	1.423
ISOTROPIC MODEL		
$E_{cortical}$ [MPa]	16,000	6500
ν	0.260	0.300
TRANSVERSELY ISOTROPIC MODEL		
$E_1 = E_2$ [MPa]	11,000	5500
E_3 [MPa]	16,000	6400
G_{12} [MPa]	4370	3500
$G_{13} = G_{23}$ [MPa]	6350	2540
$\nu_{12} = \nu_{13} = \nu_{23}$	0.260	0.300

Table 7 summarizes the experimentally measured and numerically predicted eigenfrequencies, both before and after material parameter updating, together with the corresponding frequency errors and MAC values relative to the experimental results.

Table 7. Obtained results of the eigenfrequencies for experimental modal analysis and both numerical models before and after parameter updating.

Experimental vs. Updated Numerical Model										
Mode Number	**1**	**2**	**3**	**4**	**5**	**6**	**7**	**8**	**9**	**10**
EMA [Hz]	**1999**	**2580**	**3527**	**3752**	**4233**	**4877**	**5494**	**5835**	**6433**	**7031**
ISOTROPIC MODEL										
FE before updating [Hz]	2924	3624	4654	5533	5796	6651	7449	7651	8002	8328
Error [%]	46.25	40.48	31.95	47.45	36.91	36.37	35.59	31.12	24.39	18.44
MAC value	0.878	0.851	0.720	0.794	0.617	0.008	0.048	0.037	0.211	0.005
FE after updating [Hz]	2025	2538	3285	3843	4092	4656	5213	5308	5731	5899
Error [%]	1.29	−1.62	−6.86	2.41	−3.34	−4.53	−5.11	−9.04	−10.91	−16.11
MAC value	0.886	0.853	0.769	0.728	0.523	0.011	0.098	0.013	0.196	0.073
TRANSVERSELY ISOTROPIC MODEL										
FE before updating [Hz]	2708	3334	4245	4995	5108	6151	6678	6905	7200	7645
Error [%]	35.45	29.23	20.35	33.11	20.66	26.12	21.56	18.33	11.92	8.73
MAC value	0.885	0.862	0.607	0.831	0.646	0.005	0.068	0.023	0.259	0.019
FE after updating [Hz]	2022	2566	3256	3846	4143	4739	5207	5360	5659	5900
Error [%]	1.14	−0.53	−7.69	2.49	−2.13	−2.83	−5.22	−8.15	−12.03	−16.09
MAC value	0.885	0.856	0.738	0.739	0.501	0.014	0.055	0.029	0.146	0.107

For the isotropic model, the average eigenfrequency error was reduced from 34.90% to 6.12%, whereas for the transversely isotropic model it decreased from 22.55% to 5.83%. Owing to the stronger MAC correlation observed for the first five modes, these modes were used as the primary drivers in the material updating process. For these modes, the average error was reduced from 40.61% to 3.10% for the isotropic model and from 27.76% to 2.80% for the transversely isotropic model. These improvements were achieved without substantially affecting the MAC values for the most relevant modes, namely modes 1 through 5. Higher-mode discrepancies were expected due to excitation and identification limitations.

A comparison between the isotropic and transversely isotropic models shows that the latter provides a consistently better match to the experimental results. This confirms that the transversely isotropic model offers a more accurate representation of the physical

specimen and aligns more closely with the expected orientation-dependent behaviour arising from the glass-fibre distribution in the epoxy matrix. Finally, Figure 6 illustrates the agreement between the experimental mode shapes and those predicted by the updated transversely isotropic FE model.

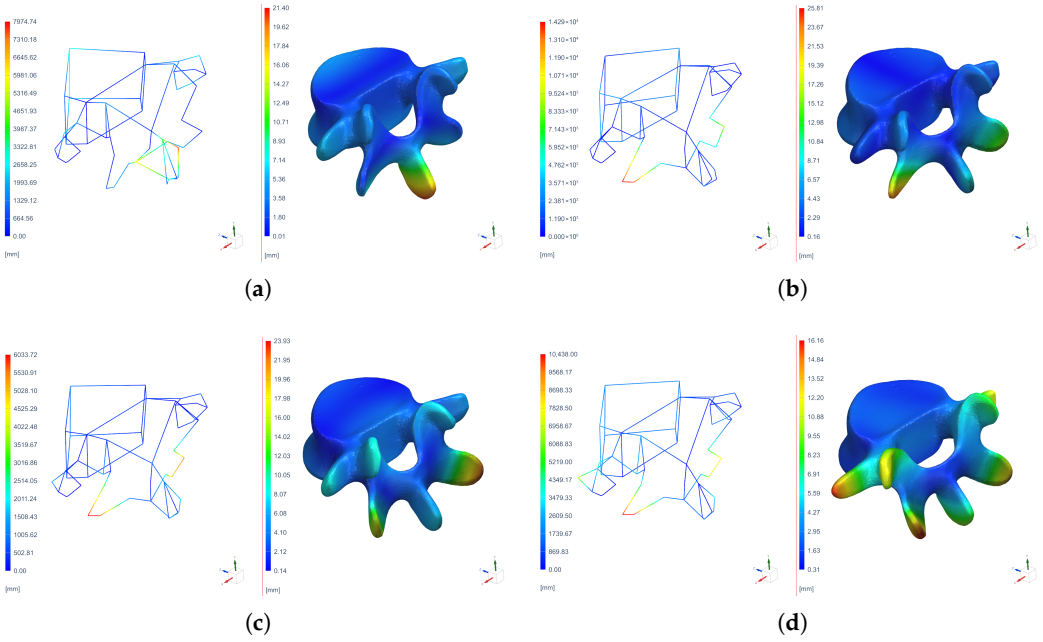

Figure 6. Comparison of the first 4 modes (first mode (**a**); second mode (**b**); third mode (**c**); fourth mode (**d**)) between the experimental modal analysis and the updated transversely isotropic FE model. The numerical mode shapes were retrieved from the FE software, while the experimental mode shapes were obtained from Testlab using the established geometry. Both are represented in magnitude, shown with colour and scale, while the direction is represented as a deviation from the original shape.

4. Discussion

This study identified the elastic material properties of a fourth-generation composite L5 vertebra replica (Sawbones Model 3429-5, Sawbones, Vashon Island, WA, USA) using a non-invasive, modal-analysis-based approach. To this end, a FE model updating strategy was used, similar to [17], in which experimentally obtained modal parameters (natural frequencies and mode shapes) from EMA were used as reference data. The elastic material parameters of the numerical model were iteratively adjusted until a satisfactory correlation between the numerical and experimental modal characteristics was achieved.

Mechanical testing methods such as compression, bending, torsion and indentation tests have traditionally been considered the gold standard for biomechanical characterization and determination of bone elastic properties. However, these methods are less suitable for geometrically complex structures such as the vertebra and inherently compromise structural integrity. Modal-based FE updating using experimental vibration data, widely adopted in civil engineering, has proven successful for FE model validation and elastic material parameter identification in anatomical composite bone models [16,17,28] and cadaveric specimens [29–33]. Reported applications include the characterization of composite Sawbones models of the femur, tibia [16], clavicle [17], and pelvis [34], which primarily concern long bones with approximately cylindrical geometry or large flat bone geometries. Complementing the existing state-of-the-art, the present study extends the methodology to a composite L5 vertebra by validating its FE model through modal-based calibration of the elastic material constants. To the authors' knowledge, modal-based FE

updating has not yet been applied to a vertebra model or to a bone replica with comparable geometric and material complexity.

Modal-calibrated vertebral FE models can support vibration-based biomechanical research, including assessment of implant fixation stability [35–37], effects of bone quality and density distribution on dynamic response [6,38], and structural changes due to healing and degradation [39,40]. Furthermore, they provide a robust basis for numerical orthopedic analyses, such as load and stress evaluation [41], prediction of stress-shielding effects [42], and evaluation of implant-related wear mechanisms [43]. These models extend the scope of in-vitro studies by enabling systematic variation of material properties, boundary conditions, and loading scenarios that are difficult or infeasible to reproduce experimentally, supporting the optimization of surgical techniques or implant design.

The verification measurements for the sheet model showed excellent agreement with the Sawbones datasheet [19], confirming that the presented workflow accurately reproduces the manufacturer-provided material properties derived from mechanical testing of the sheet model. In contrast, the vertebra model required substantial parameter adjustments, reinforcing the conclusion that the manufacturer's datasheet material properties cannot be directly applied to complex anatomical geometries.

As a first step in the FE updating procedure for the vertebra model, the mass discrepancy between the FE model and the physical bone replica was reduced by updating the cortical bone density from 1.640 g/cm^3 to 1.423 g/cm^3, while keeping the cancellous bone density constant due to its limited contribution to the total mass. Although the discrepancy could also have been addressed by modifying the thickness of the cortical layer, density was selected as the updating parameter in this study. Uncertainties in cortical thickness representation arising from CT resolution limits or segmentation inaccuracies may partly contribute to the observed mass difference, but are unlikely to fully account for it; a shared contribution of thickness and density variability is regarded as more plausible. Therefore, density was selected as an effective updating parameter, primarily reflecting dominant uncertainties in material characterization, while implicitly accounting for potential geometric inaccuracies in the reconstructed cortical shell.

During the model updating process, only the elastic material properties of the cortical layer were adjusted, while the properties of the cancellous layer were kept constant. This choice was motivated by a prior sensitivity analysis (Tables 2 and 3). Both the cortical and cancellous layers are assumed to be homogeneous and to exhibit linear elastic behaviour. Comparison of the cortical bone analogue before and after updating reveals that substantial parameter adjustments were required to minimize discrepancies between numerical and experimental modal results. These findings are consistent with previous modal-based validation studies on Sawbones anatomical bone replicas, which generally report a reduction in longitudinal Young's modulus relative to manufacturer-provided values [16,17,28]. However, whereas those studies observed increased shear moduli and reduced Poisson's ratios, the present study yielded the opposite trends. Moreover, the magnitude of the parameter changes in this study exceeds those reported previously. For instance, while Goossens et al. reported a 20% reduction in longitudinal Young's modulus (from 16,000 MPa to 12,880 MPa) for a transversely isotropic clavicle model [17], reductions of 50% and 60% were obtained here for the transversely isotropic vertebra model. Many of these previous studies focused on long bones, whose cylindrical geometry promotes relatively uniform flow-induced fibre alignment during injection molding, and is therefore more compatible with a transversely isotropic material assumption. In contrast, the vertebra's intricate geometry likely induces heterogeneous fibre patterns during manufacturing. Although transverse isotropic behaviour with isotropy in the 1–2 plane may reasonably approximate the behaviour of the vertebral body, it is less suitable for the vertebral processes, where local geometry varies

substantially. As a result, a single global set of transversely isotropic material constants is forced to represent a structure whose effective stiffness varies locally due to shape-driven manufacturing effects, necessitating larger parameter adjustments during model updating.

To the authors' knowledge, no comparable mechanical validation data for vertebra models are available. However, previous work has shown that, for long bones, modal-based updating yields results consistent with other experimental validation studies that applied a strain based validation method [17].

Several experimental limitations must be acknowledged for the updating strategy. Based on the initial numerical analysis, the first 10 modes were expected to span a high-frequency range, extending up to approximately 8.3 kHz. To ensure adequate modal excitation of the modes, it is generally recommended that the auto-power spectrum of the hammer force does not decay by more than 20 dB over the frequency range of interest [14]. However, experimental evaluation of different hammer tips showed that, even when using the hardest available tip, the −20 dB level in the input power spectral density was reached at approximately 3.6 kHz, while the −30 dB level occurred around 4.5 kHz. This indicates that beyond this frequency range the input excitation energy is insufficient to reliably excite higher-order modes. Consequently, only the first five modes could be expected to be identified with sufficient confidence, whereas higher-order modes are likely to be less accurately estimated and should therefore be interpreted with caution. Consequently, the FE model updating procedure primarily focused on the first five modes, with particular emphasis on the first three modes, which exhibit highest experimental robustness and reliability. This focus does not necessarily represent a drawback, as lower-order modes are more representative of global elastic material properties, whereas higher-order modes are more sensitive to local structural variations and complex geometrical features of the vertebral arch.

In other studies, shaker excitation has been used for higher modal identification accuracy due to its broadband input. This was not feasible here, as attaching a shaker to the lightweight vertebra would alter its dynamic behaviour. Adding more contact sensors for more accurate modal identification was also avoided, since the lightweight nature of the structure makes it susceptible to mass-loading effects which could bias the modal parameters. While a laser Doppler vibrometer could allow denser, non-contact measurements, maintaining focus on a small, lightweight, intrecate geometry suspended by elastic cords is challenging. Despite these limitations, the first five modes were reliably identified and showed good agreement with numerical predictions, supporting the validity of the modal analysis and subsequent FE model updating.

Due to the large discrepancy between the initial FE results and the experimental measurements, combined with the high number of interdependent elastic material parameters, the optimization landscape contained multiple closely spaced local minima that yielded dynamically equivalent responses. Consequently, during several steps of the sensitivity-based updating procedure, decisions were guided by engineering knowledge and experience to approximate realistic structural behaviour as closely as possible. These decisions were based not only on the observed frequency errors and MAC values, but also on the deformation behaviour and the physical plausibility of the updated material properties. For example, a comparable reduction in frequency error could be achieved by drastically modifying only two parameters. Although such a local minimum may exhibit seemingly good agreement with the EMA results, it lacks physical justification from an engineering perspective, and leads to compromises in the MAC matrix, thereby reducing the model reliability.

In this study, the cancellous analogue was modelled as isotropic, whereas the cortical analogue was simulated as both isotropic and transversely isotropic material in two separate

updating studies. Given that Sawbones composite models are manufactured via injection moulding, fibre orientation could be influenced by flow patterns during processing and becomes increasingly difficult to control in components with complex geometries [20]. Accordingly, an isotropic material model was first adopted, assuming a quasi-random fibre distribution. A second approach assumed preferential fibre alignment along the cranio–caudal direction, motivating transversely isotropic material behaviour. Both the isotropic and transversely isotropic FE models showed significant improvements after material parameter updating; however, from the results it could be seen that the FE model with the transversely isotropic cortical layer consistently achieved the best agreement with the experimental modal data. This observation aligns with prior studies demonstrating the importance of directional material behaviour for accurately modelling the dynamic response of composite bone models [16]. Given the manufacturing process of the vertebral models, future studies may further improve model fidelity by introducing element-specific material orientations within the cortical layer, assigning the transverse elastic modulus to the direction normal to the element surface and the longitudinal elastic modulus to the in-plane directions.

This study only tested one composite vertebra bone model. Nonetheless, a low inter-specimen variability is documented for fourth-generation Sawbones models, with only 0.9% up to 9.3% for tibia models [16,44,45], and 0.8% up to 7.5% for femur models [16,45].

Future research will focus on applying the same method to test vertebra models from different manufacturers. This would enable a systematic comparison of their characteristics and mechanical representativeness with respect to human bone, thereby supporting more informed model selection for biomechanical research applications.

5. Conclusions

This study presents two updated finite element models of a composite L5 vertebra: one fully isotropic and one combining an isotropic cancellous layer with a transversely isotropic cortical layer. The used approach of modal-based FE updating using experimental vibration data has been applied for long bones and large flat bones in the past; the novelty of this paper is that it is now applied to a more complex anatomical structure, namely a lumbar vertebra model.

After updating the material properties using experimental modal analysis, both models show a substantial improvement in agreement with experimental results. For the isotropic model, the average eigenfrequency error was reduced from 34.90% to 6.12% for all modes and from 40.61% to 3.10% for the first five modes. For the transversely isotropic model, the corresponding errors decreased from 22.55% to 5.83% and from 27.76% to 2.80%, respectively. These results demonstrate that the updated models provide accurate and reliable numerical representations of a fourth-generation Sawbones composite L5 vertebra, suitable for future studies on the bone model's mechanical and dynamic behaviour. The updated material properties and the documented workflow provide a robust foundation for vibration-based biomechanical research and numerical orthopaedic analyses, and can be readily adopted to support implant fixation studies as well as comparative studies across composite bone manufacturers.

Author Contributions: Conceptualization, M.V.d.B., H.D.V.d.S., M.T., K.G. and K.D.; methodology, M.V.d.B., H.D.V.d.S., M.T. and K.D.; formal analysis, M.V.d.B., H.D.V.d.S., M.T. and K.D.; investigation, M.V.d.B., H.D.V.d.S. and M.T.; writing—original draft preparation, M.V.d.B., H.D.V.d.S. and M.T.; writing—review and editing, K.D. and K.G.; visualization, M.V.d.B., H.D.V.d.S. and M.T.; supervision, K.D. and K.G. All authors have read and agreed to the published version of the manuscript.

Funding: This research was funded by KU Leuven Internal Funding and FWO Vlaanderen under grant number 1S35424N.

Institutional Review Board Statement: Not applicable.

Informed Consent Statement: Not applicable.

Data Availability Statement: The original contributions presented in this study are included in the article. The raw data supporting the conclusions of this article will be made available by the authors on request.

Conflicts of Interest: The authors declare no conflicts of interest. The funders had no role in the design of the study; in the collection, analyses, or interpretation of data; in the writing of the manuscript; or in the decision to publish the results.

References

1. Grover, P.; Albert, C.; Wang, M.; Harris, G. Mechanical characterization of fourth generation composite humerus. *Proc. Inst. Mech. Eng. Part H J. Eng. Med.* **2011**, *225*, 1169–1176. [CrossRef]
2. Saunders, M. *Mechanical Testing for the Biomechanics Engineer: A Practical Guide*; Springer: Cham, Switzerland, 2015. [CrossRef]
3. Reed, J.D.; Stanbury, S.J.; Menorca, R.M.; Elfar, J.C. The emerging utility of composite bone models in biomechanical studies of the hand and upper extremity. *J. Hand Surg.* **2013**, *38*, 583–587. [CrossRef]
4. Zdero, R.; Brzozowski, P.; Schemitsch, E.H. Biomechanical properties of artificial bones made by sawbones: A review. *Med. Eng. Phys.* **2023**, *118*, 104017. [CrossRef]
5. Elfar, J.J.; Menorca, R.M.G.; Reed, J.D.; Stanbury, S. Composite bone models in orthopaedic surgery research and education. *J. Am. Acad. Orthop. Surg.* **2014**, *22*, 111–120. [PubMed]
6. Meslier, Q.A.; Shefelbine, S.J. Using finite element modeling in bone mechanoadaptation. *Curr. Osteoporos. Rep.* **2023**, *21*, 105–116. [CrossRef]
7. Zhang, S.; Bai, T.; Zhang, X.; Feng, C.; Liu, Z.; Zhang, Y. Application of finite element analysis in biomechanical research of degenerative diseases of lumbar spine. *J. Biosci. Med.* **2022**, *10*, 21–33. [CrossRef]
8. Yan, M.; Liang, T.; Zhao, H.; Bi, Y.; Wang, T.; Yu, T.; Zhang, Y. Model properties and clinical application in the finite element analysis of knee joint: A review. *Orthop. Surg.* **2024**, *16*, 289–302. [CrossRef]
9. Dickinson, A.; Taylor, A.; Ozturk, H.; Browne, M. Experimental validation of a finite element model of the proximal femur using digital image correlation and a composite bone model. *J. Biomech. Eng.* **2011**, *133*, 14504. [CrossRef] [PubMed]
10. Goshulak, P.; Samiezadeh, S.; Aziz, M.S.; Bougherara, H.; Zdero, R.; Schemitsch, E.H. The biomechanical effect of anteversion and modular neck offset on stress shielding for short-stem versus conventional long-stem hip implants. *Med. Eng. Phys.* **2016**, *38*, 232–240. [CrossRef] [PubMed]
11. Gee, A.; Bougherara, H.; Schemitsch, E.H.; Zdero, R. Biomechanical design using in-vitro finite element modeling of distal femur fracture plates made from semi-rigid materials versus traditional metals for post-operative toe-touch weight-bearing. *Med. Eng. Phys.* **2020**, *87*, 95. [CrossRef]
12. Turbucz, M.; Pokorni, A.J.; Szőke, G.; Hoffer, Z.; Kiss, R.M.; Lazary, A.; Eltes, P.E. Development and validation of two intact lumbar spine finite element models for in silico investigations: Comparison of the bone modelling approaches. *Appl. Sci.* **2022**, *12*, 10256. [CrossRef]
13. Wirtz, D.C.; Schiffers, N.; Pandorf, T.; Radermacher, K.; Weichert, D.; Forst, R. Critical evaluation of known bone material properties to realize anisotropic FE-simulation of the proximal femur. *J. Biomech.* **2000**, *33*, 1325–1330. [CrossRef]
14. Heylen, W.; Sas, P. *Modal Analysis Theory and Testing*; Katholieke Universteit Leuven: Leuven, Belgium, 2006.
15. Kurent, B.; Ao, W.K.; Pavic, A.; Pérez, F.; Brank, B. Modal testing and finite element model updating of full-scale hybrid timber-concrete building. *Eng. Struct.* **2023**, *289*, 116250. [CrossRef]
16. Leuridan, S.; Goossens, Q.; Pastrav, L.; Roosen, J.; Mulier, M.; Denis, K.; Desmet, W.; Vander Sloten, J. Determination of replicate composite bone material properties using modal analysis. *J. Mech. Behav. Biomed. Mater.* **2017**, *66*, 12–18. [CrossRef]
17. Goossens, Q.; Vancleef, S.; Leuridan, S.; Pastrav, L.C.; Mulier, M.; Desmet, W.; Vander Sloten, J.; Denis, K. The use of a vibro-acoustic based method to determine the composite material properties of a replicate clavicle bone model. *J. Funct. Biomater.* **2020**, *11*, 69. [CrossRef]
18. Sawbones. Absolute™ (Short Fiber Filled Epoxy) Properties. Available online: https://sawbones.com/absolute-properties/ (accessed on 24 December 2025).
19. Sawbones. Test Materials and Composite Bones. Biomechanical Products Catalog. 2020. Available online: https://pdf.medicalexpo.com/pdf/sawbones-pacific-research-labs/biomechanical-test-materials/103604-179595.html (accessed on 24 December 2025).

20. Żurawik, R.; Volke, J.; Zarges, J.C.; Heim, H.P. Comparison of real and simulated fiber orientations in injection molded short glass fiber reinforced polyamide by X-ray microtomography. *Polymers* **2021**, *14*, 29. [CrossRef]
21. Wang, T.; Ball, J.R.; Pelletier, M.H.; Walsh, W.R. Biomechanical evaluation of a biomimetic spinal construct. *J. Exp. Orthop.* **2014**, *1*, 3. [CrossRef] [PubMed]
22. Menachem, S.; Seex, K. A biomechanical study shows the direction of compression influences the amount of lordosis gained in lumbar fusion. *Clin. Biomech.* **2023**, *101*, 105862. [CrossRef]
23. Sawbones. Lumbar L5, Absolute™ 4th Gen. With 10 PCF Solid Foam Cancellous. 2025. Available online: https://sawbones.com/products/lumbar-l5-absolute-4th-gen-with-10-pcf-solid-foam-cancellous.html (accessed on 24 December 2025).
24. Sawbones. Solid Rigid Polyurethane Foam Properties. Available online: https://sawbones.com/solid-rigid-polyurethane-foam-properties/ (accessed on 24 December 2025).
25. Carne, T.G.; Griffith, D.; Casias, M.E. *Support Conditions for Free Boundary-Condition Modal Testing*; Technical Report; Sandia National Lab. (SNL-NM): Albuquerque, NM, USA, 2006.
26. O'donoughue, P.; Gautier, F.; Meteyer, E.; Durand-Texte, T.; Secail-Geraud, M.; Foucart, F.; Robin, O.; Berry, A.; Melon, M.; Pézerat, C.; et al. Comparison of three full-field optical measurement techniques applied to vibration analysis. *Sci. Rep.* **2023**, *13*, 3261. [CrossRef]
27. Weekes, B.; Ewins, D. Effective use of scanning laser doppler vibrometers for modal testing. In *Proceedings of the Topics in Modal Analysis II, Volume 8: Proceedings of the 32nd IMAC, A Conference and Exposition on Structural Dynamics*; Springer: Cham, Switzerland, 2014; pp. 43–58.
28. Timmermans, M.; Makris, G.A.; Goossens, Q.; Pastrav, L.; Desmet, W.; Denis, K. Experimental Modal Analysis for the Determination of Bone Replicate Material Properties. In Proceedings of the 26th Congress of the European Society of Biomechanics (ESB 2021), Milan, Italy, 11–14 July 2021.
29. Taylor, W.; Roland, E.; Ploeg, H.; Hertig, D.; Klabunde, R.; Warner, M.; Hobatho, M.; Rakotomanana, L.; Clift, S. Determination of orthotropic bone elastic constants using FEA and modal analysis. *J. Biomech.* **2002**, *35*, 767–773. [CrossRef]
30. Neugebauer, R.; Werner, M.; Voigt, C.; Steinke, H.; Scholz, R.; Scherer, S.; Quickert, M. Experimental modal analysis on fresh-frozen human hemipelvic bones employing a 3D laser vibrometer for the purpose of modal parameter identification. *J. Biomech.* **2011**, *44*, 1610–1613. [CrossRef]
31. Hobatho, M.C.; Darmana, R.; Pastor, P.; Barrau, J.J.; Laroze, S.; Morucci, J.P. Development of a three-dimensional finite element model of a human tibia using experimental modal analysis. *J. Biomech.* **1991**, *24*, 371–383. [CrossRef]
32. Bernard, S.; Grimal, Q.; Laugier, P. Accurate measurement of cortical bone elasticity tensor with resonant ultrasound spectroscopy. *J. Mech. Behav. Biomed. Mater.* **2013**, *18*, 12–19. [CrossRef]
33. Semaan, M.; Mora, P.; Bernard, S.; Launay, F.; Payan, C.; Lasaygues, P.; Pithioux, M.; Baron, C. Assessment of elastic coefficients of child cortical bone using resonant ultrasound spectroscopy. *J. Mech. Behav. Biomed. Mater.* **2019**, *90*, 40–44. [CrossRef]
34. Henyš, P.; Čapek, L. Material model of pelvic bone based on modal analysis: A study on the composite bone. *Biomech. Model. Mechanobiol.* **2017**, *16*, 363–373. [CrossRef] [PubMed]
35. Leuridan, S.; Goossens, Q.; Vander Sloten, T.; De Landsheer, K.; Delport, H.; Pastrav, L.; Denis, K.; Desmet, W.; Vander Sloten, J. Vibration-based fixation assessment of tibial knee implants: A combined in vitro and in silico feasibility study. *Med. Eng. Phys.* **2017**, *49*, 109–120. [CrossRef] [PubMed]
36. Henyš, P.; Leuridan, S.; Goossens, Q.; Mulier, M.; Pastrav, L.; Desmet, W.; Vander Sloten, J.; Denis, K.; Čapek, L. Modal frequency and shape curvature as a measure of implant fixation: A computer study on the acetabular cup. *Med. Eng. Phys.* **2018**, *60*, 30–38. [CrossRef] [PubMed]
37. Poudrel, A.S.; Bouffandeau, A.; Rosi, G.; Dubory, A.; Lachaniette, C.H.F.; Nguyen, V.H.; Haiat, G. 3-D finite element model of the impaction of a press-fitted femoral stem under various biomechanical environments. *Comput. Biol. Med.* **2024**, *174*, 108405. [CrossRef]
38. Poudrel, A.S.; Nguyen, V.H.; Rosi, G.; Haiat, G. Influence of the biomechanical environment on the femoral stem insertion and vibrational behavior: A 3-D finite element study. *Biomech. Model. Mechanobiol.* **2023**, *22*, 611–628. [CrossRef]
39. Liu, C.; Wang, S.; Zhao, Y.; Shen, Y.; Zhang, M.; Li, H.; Wang, Y.; Xue, Y.; Wu, X.; Chen, W.; et al. Design of a porous biodegradable internal fixation for the treatment of pauwels type III femoral neck fractures. *Front. Bioeng. Biotechnol.* **2025**, *13*, 1639459. [CrossRef]
40. Ketata, H.; Kharrat, M.; Dammak, M. Modeling age-related changes in the mechanical behavior of the fracture-fixated human tibia bone during healing. *Med. Eng. Phys.* **2020**, *81*, 77–85. [CrossRef]
41. Xiao, Y.; He, K.; Tan, X.; Wei, D.; Yan, J.; Yang, Y.; Xiang, F. Biomechanical evaluation of implant techniques for ipsilateral femoral neck and shaft fractures: A finite element analysis. *J. Mech. Behav. Biomed. Mater.* **2025**, *164*, 106890. [CrossRef]
42. Mori, Y.; Tanaka, H.; Kurishima, H.; Kanabuchi, R.; Mori, N.; Sasagawa, K.; Aizawa, T. Biomechanical and Clinical Validation of a Modulus-Graded Ti-Nb-Sn Femoral Stem for Suppressing Stress Shielding in Total Hip Arthroplasty. *Appl. Sci.* **2025**, *15*, 4827. [CrossRef]

43. Lee, H.K.; Kim, S.M.; Lim, H.S. Computational wear prediction of TKR with flatback deformity during gait. *Appl. Sci.* **2022**, *12*, 3698. [CrossRef]
44. Cristofolini, L.; Viceconti, M. Mechanical validation of whole bone composite tibia models. *J. Biomech.* **2000**, *33*, 279–288. [CrossRef] [PubMed]
45. Heiner, A.D. Structural properties of fourth-generation composite femurs and tibias. *J. Biomech.* **2008**, *41*, 3282–3284. [CrossRef]

Disclaimer/Publisher's Note: The statements, opinions and data contained in all publications are solely those of the individual author(s) and contributor(s) and not of MDPI and/or the editor(s). MDPI and/or the editor(s) disclaim responsibility for any injury to people or property resulting from any ideas, methods, instructions or products referred to in the content.